

REPORT DOCUMENTATION PAGE			Form Approved OMB NO. 0704-0188		
<p>The public reporting burden for this collection of information is estimated to average 1 hour per response, including the time for reviewing instructions, searching existing data sources, gathering and maintaining the data needed, and completing and reviewing the collection of information. Send comments regarding this burden estimate or any other aspect of this collection of information, including suggestions for reducing this burden, to Washington Headquarters Services, Directorate for Information Operations and Reports, 1215 Jefferson Davis Highway, Suite 1204, Arlington VA, 22202-4302. Respondents should be aware that notwithstanding any other provision of law, no person shall be subject to any penalty for failing to comply with a collection of information if it does not display a currently valid OMB control number. PLEASE DO NOT RETURN YOUR FORM TO THE ABOVE ADDRESS.</p>					
1. REPORT DATE (DD-MM-YYYY) 30-07-2015		2. REPORT TYPE Final Report		3. DATES COVERED (From - To) 1-May-2011 - 30-Apr-2015	
4. TITLE AND SUBTITLE Final Report: Novel Polymers for High Efficiency Renewable and Portable Power Applications			5a. CONTRACT NUMBER W911NF-11-1-0158		
			5b. GRANT NUMBER		
			5c. PROGRAM ELEMENT NUMBER 206022		
6. AUTHORS Sam-Shajing Sun			5d. PROJECT NUMBER		
			5e. TASK NUMBER		
			5f. WORK UNIT NUMBER		
7. PERFORMING ORGANIZATION NAMES AND ADDRESSES Norfolk State University 700 Park Avenue McDemmond Center for Applied Research, Suite 601 Norfolk, VA 23504 -8060			8. PERFORMING ORGANIZATION REPORT NUMBER		
9. SPONSORING/MONITORING AGENCY NAME(S) AND ADDRESS (ES) U.S. Army Research Office P.O. Box 12211 Research Triangle Park, NC 27709-2211			10. SPONSOR/MONITOR'S ACRONYM(S) ARO		
			11. SPONSOR/MONITOR'S REPORT NUMBER(S) 58948-CH-REP.19		
12. DISTRIBUTION AVAILABILITY STATEMENT Approved for Public Release; Distribution Unlimited					
13. SUPPLEMENTARY NOTES The views, opinions and/or findings contained in this report are those of the author(s) and should not be construed as an official Department of the Army position, policy or decision, unless so designated by other documentation.					
14. ABSTRACT This research revealed several important or critical information: 1) Too much LUMO offset or electron transfer driving force between the polymer and dye would result in weaker PL quenching and optoelectronic device power conversion efficiency, this experimentally confirmed some earlier theoretical speculation or prediction and could become another evidence for the "inverted" region of Marcus electron transfer model. The results could be very useful for materials design for developing high efficiency organic and polymer based optoelectronic devices; 2) Optimum LUMO offset or highest PL quenching process much more critical than molar absorption coefficient for					
15. SUBJECT TERMS Conjugated polymers, dyes, frontier orbitals, HOMOs, LUMOs, energy gaps, photoelectric, thermoelectric, energy conversions, charge transfer, energy transfer, photoluminescence (PL).					
16. SECURITY CLASSIFICATION OF:		17. LIMITATION OF ABSTRACT UU	15. NUMBER OF PAGES	19a. NAME OF RESPONSIBLE PERSON Sam-Shajing Sun	
a. REPORT UU	b. ABSTRACT UU			c. THIS PAGE UU	19b. TELEPHONE NUMBER 757-823-2993

Report Title

Final Report: Novel Polymers for High Efficiency Renewable and Portable Power Applications

ABSTRACT

This research revealed several important or critical information: 1) Too much LUMO offset or electron transfer driving force between the polymer and dye would result in weaker PL quenching and optoelectronic device power conversion efficiency, this experimentally confirmed some earlier theoretical speculation or prediction and could become another evidence for the “inverted” region of Marcus electron transfer model. The results could be very useful for materials design for developing high efficiency organic and polymer based optoelectronic devices; 2) Optimum LUMO offset or highest PL quenching appears much more critical than molar absorption coefficient for polymer-dye based optoelectronic conversion efficiency. 3) The optoelectronic performance of covalent attached polymer-dye system is much better than the polymer/dye blend system, this could be attributed to more convenient reach of polymer/dye interface of photo generated excitons in the covalent system resulting in more efficient exciton dissociations. 4) For thermoelectric studies, it appears the thermoelectric charge carrier generations of the four conjugated polymers doped with iodine at room temperature are in the normal region of the Marcus electron transfer model. An optimal thermoelectric charge generation condition may be identified with further decreasing the orbital offsets (D-HOMO/A-LUMO) of the D/A pairs or increasing the temperature, or both

Enter List of papers submitted or published that acknowledge ARO support from the start of the project to the date of this printing. List the papers, including journal references, in the following categories:

(a) Papers published in peer-reviewed journals (N/A for none)

<u>Received</u>	<u>Paper</u>
07/29/2015 10.00	Tanya M. S. David, Cheng Zhang, Sam-Shajing Sun. Development of Low Energy Gap and Fully Regioregular Polythienylenevinylene Derivative, Journal of Chemistry, (06 2014): 1. doi: 10.1155/2014/379372
07/29/2015 12.00	Tanya M. S. David, Wondwossen Arasho, Sam-Shajing Sun. Synthesis and structure-optoelectronic property relationships of a series of PPV and SFTV derived polymers, Journal of Polymer Science Part A: Polymer Chemistry, (06 2015): 0. doi: 10.1002/pola.27703
07/30/2015 15.00	Sam-Shajing Sun, Jaleesa Brooks, Thuong Nguyen, Amanda Harding, Dan Wang, Tanya David. Novel Organic and Polymeric Materials for Solar Energy Conversions, Energy Procedia, (10 2014): 79. doi: 10.1016/j.egypro.2014.10.011
07/30/2015 18.00	Jianyuan Sun, Logan P. Sanow, Sam-Shajing Sun, Cheng Zhang. Dicyano-Substituted Poly (phenylenevinylene) (DiCN-PPV) and the Effect of Cyano Substitution on Photochemical Stability, Macromolecules, (06 2013): 4247. doi: 10.1021/ma400661f
08/10/2012 1.00	Tanya David, Jaleesa Brooks, Thuong Nguyen, Sam-Shajing Sun, Cheng Zhang, Rui Li. Frontier orbital and morphology engineering of conjugated polymers and block copolymers for potential high efficiency photovoltaics, Solar Energy Materials and Solar Cells, (02 2012): 150. doi: 10.1016/j.solmat.2011.09.040
08/30/2014 6.00	Sam-Shajing Sun, Jaleesa Brooks, Thuong Nguyen, Cheng Zhang. Design, synthesis, and characterization of a novel c-donor-nc-bridge-c-acceptor type block copolymer for optoelectronic applications, Journal of Polymer Science Part A: Polymer Chemistry, (04 2014): 1149. doi: 10.1002/pola.27098
TOTAL:	6

Number of Papers published in peer-reviewed journals:

(b) Papers published in non-peer-reviewed journals (N/A for none)

Received Paper

TOTAL:

Number of Papers published in non peer-reviewed journals:

(c) Presentations

Number of Presentations: 2.00

Non Peer-Reviewed Conference Proceeding publications (other than abstracts):

Received Paper

07/30/2015 17.00 Dan Wang, Sam Sun. Optoelectronic Properties of A Series of P3HT/Dye Composites, 247th American Chemical Society National Convention. 16-MAR-14, . . . ,

08/20/2013 5.00 Amanda Harding, Samshajing Sun. Optoelectronic Properties of ttb-ZnPc/rr-P3HT Composite, Amercian Chemical Society National Convention. 11-APR-13, . . . ,

TOTAL: 2

Number of Non Peer-Reviewed Conference Proceeding publications (other than abstracts):

Peer-Reviewed Conference Proceeding publications (other than abstracts):

<u>Received</u>	<u>Paper</u>
07/29/2015 9.00	Sam-Shajing Sun, Wondwossen Arasho, Tanya David. Engineering polymer frontier orbitals for efficient photon harvesting, SPIE Optical Engineering + Applications. 17-AUG-14, San Diego, California, United States. : ,
07/29/2015 11.00	Sam-Shajing Sun, Thuong Nguyen, Jaleesa Brooks. Fluorinated polyphenylenevinylene (PPV) block copolymers for nanophotonics, SPIE Optical Engineering + Applications. 25-AUG-13, San Diego, California, United States. : ,
07/30/2015 16.00	S. Sun, T. Nguyen, M. Hasib, D. Wang. Polymer Nanostructure Approach for Photoelectric Solar Energy Conversions, TechConnect World Innovation Conference. 17-JUN-15, . : ,
08/10/2012 2.00	Sam-Shajing Sun, Thuong Nguyen, Jaleesa Brooks,, Amanda Harding, Eumee Song, Tanya David, Cheng Zhang. Polymer Frontier Orbital and Morphology Engineering for Nanophotonics, Nanophotonics and Macrophotonics for Space Environments VI. 13-AUG-12, . : ,
08/20/2013 3.00	Sam-Shajing Sun, Thuong Nguyen, Jaleesa Brooks, Amanda Harding, Eumee Song, Tanya David, Cheng Zhang. Polymer frontier orbital and morphology engineering for nanophotonics, SPIE Optical Engineering + Applications. 16-AUG-12, San Diego, California, USA. : ,
TOTAL:	5

Number of Peer-Reviewed Conference Proceeding publications (other than abstracts):

(d) Manuscripts

<u>Received</u>	<u>Paper</u>
07/29/2015 13.00	Sam-Shajing Sun , Dan Wang. Polymer Light Harvesting Composites for Optoelectronic Applications, Nanophotonics and Macrophotonics for Space Environments XV, 2015, Vol. 9616 (07 2015)
08/20/2013 4.00	Jianyuan Sun, Logan P. Sanow, Sam-Shajing Sun, Cheng Zhang. Dicyano-Substituted Poly (phenylenevinylene) (DiCN?PPV) and theEffect of Cyano Substitution on Photochemical Stability, Macromoleculcs (04 2013)
08/30/2014 8.00	Sam-Shajing Sun, Jaleesa Brooks, Thuong Nguyen, Amanda Harding, Dan Wang, and Tanya David. Novel Organic and Polymeric Materials for Solar Energy Applications, Energy Procedia (12 2013)
TOTAL:	3

Number of Manuscripts:

Books

Received Book

TOTAL:

Received Book Chapter

07/29/2015 14.00 Sam-Shajing Sun. Chapter 3: Basic Electronic Structures and Charge Carrier Generation in Organic Optoelectronic Materials , Boca Raton, FL, USA: CRC Press, (12 2015)

08/30/2014 7.00 Samshajing Sun, Amanda Harding. Dye Sensitized Polymer Composites for Sunlight Harvesting, United States: American Chemical Society, (10 2014)

TOTAL: 2

Patents Submitted

Patents Awarded

Awards

Graduate Students

<u>NAME</u>	<u>PERCENT SUPPORTED</u>	Discipline
Whitney Lagrone	0.00	
Dan Wang	0.00	
Tanya David	0.00	
Amanda Harding	0.00	
Muhammad Hasib	0.00	
Meric Arslan	0.00	
Jaleesa Brooks	0.00	
Thuong Nguyen	0.00	
FTE Equivalent:	0.00	
Total Number:	8	

Names of Post Doctorates

<u>NAME</u>	<u>PERCENT SUPPORTED</u>
FTE Equivalent:	
Total Number:	

Names of Faculty Supported

<u>NAME</u>	<u>PERCENT SUPPORTED</u>	National Academy Member
Sam-Shajing Sun	0.00	
FTE Equivalent:	0.00	
Total Number:	1	

Names of Under Graduate students supported

<u>NAME</u>	<u>PERCENT SUPPORTED</u>
FTE Equivalent:	
Total Number:	

Student Metrics

This section only applies to graduating undergraduates supported by this agreement in this reporting period

The number of undergraduates funded by this agreement who graduated during this period: 2.00

The number of undergraduates funded by this agreement who graduated during this period with a degree in science, mathematics, engineering, or technology fields:..... 2.00

The number of undergraduates funded by your agreement who graduated during this period and will continue to pursue a graduate or Ph.D. degree in science, mathematics, engineering, or technology fields:..... 2.00

Number of graduating undergraduates who achieved a 3.5 GPA to 4.0 (4.0 max scale):..... 2.00

Number of graduating undergraduates funded by a DoD funded Center of Excellence grant for Education, Research and Engineering:..... 0.00

The number of undergraduates funded by your agreement who graduated during this period and intend to work for the Department of Defense 0.00

The number of undergraduates funded by your agreement who graduated during this period and will receive scholarships or fellowships for further studies in science, mathematics, engineering or technology fields:..... 2.00

Names of Personnel receiving masters degrees

<u>NAME</u> Whitney Lagrone Dan Wang Jaleesa Brooks Total Number: 3
--

Names of personnel receiving PHDs

<u>NAME</u> Tanya David Thuong Nguyen Total Number: 2

Names of other research staff

<u>NAME</u>	<u>PERCENT SUPPORTED</u>
FTE Equivalent:	
Total Number:	

Sub Contractors (DD882)

Inventions (DD882)

Scientific Progress

This research revealed several important or critical information: 1) Too much LUMO offset or electron transfer driving force between the polymer and dye would result in weaker PL quenching and optoelectronic device power conversion efficiency, this experimentally confirmed some earlier theoretical speculation or prediction and could become another evidence for the "inverted" region of Marcus electron transfer model. The results could be very useful for materials design for developing high efficiency organic and polymer based optoelectronic devices; 2) Optimum LUMO offset or highest PL quenching appears much more critical than molar absorption coefficient for polymer-dye based optoelectronic conversion efficiency. 3) The optoelectronic performance of covalent attached polymer-dye system is much better than the polymer/dye blend system, this could be attributed to more convenient reach of polymer/dye interface of photo generated excitons in the covalent system resulting in more efficient exciton dissociations. 4) For thermoelectric studies, it appears the thermoelectric charge carrier generations of the four conjugated polymers doped with iodine at room temperature are in the normal region of the Marcus electron transfer model. An optimal thermoelectric charge generation condition may be identified with further decreasing the orbital offsets (D-HOMO/A-LUMO) of the D/A pairs or increasing the temperature, or both

Technology Transfer

Final Project Report (FPR)

“Novel Polymers for High Efficiency Renewable and Portable Power Applications”

ARO Award #: W911-NF11-1-0158

PI: Sam Sun, Ph.D.
Professor of Chemistry and Materials Science
Ph.D. Program in Materials Science and Engineering
Department of Chemistry and Center for Materials Research
Norfolk State University
700 Park Avenue, Norfolk, VA 23504
Tel: 757-823-2993; Email: ssun@nsu.edu

July 2015

1. TABLE OF CONTENTS

1. TABLE OF CONTENTS	1
2. LIST OF ILLUSTRATIONS AND TABLES	2
3. STATEMENT OF THE PROBLEMS STUDIED	4
3.1 Project Research Objectives.....	4
3.2 Project Research Approaches	4
3.3 Project Challenges.....	4
4. SUMMARY OF MOST IMPORTANT RESULTS.....	5
4.1 Important Results On Photoelectric Studies	5
4.2 Important Results On Thermoelectric Studies	20
4.3 Student Training/Education/Publication Accomplishments.....	25
5. BIBLIOGRAPHY	26

2. LIST OF ILLUSTRATIONS AND TABLES

Figure 1. Scheme of molecular frontier orbitals and photo-induced charge transfer (CT) processes in an organic donor/acceptor binary light harvesting system.	5
Figure 2. Scheme of standard Gibbs free-energy potential wells of photo-induced charge transfer processes in an organic donor/acceptor light harvesting system.	6
Figure 3. Scheme of photo induced exciton dissociation (or exciton quenching parameter, $Y_{eq(D+A)}$, middle solid curve), germinate charge recombination rate constant (K_r , left long dashed curve), and charge recombination quenching parameter ($Y_{rq(D+A)}$, right short dashed curve) versus LUMO offsets (δE) of a PPV based D/A pair [2-3].	6
Figure 4. Frontier orbital schemes of (a) proposed dye molecular units (MUs) sensitized triple-component organic photoelectric systems and (b) organic donor/acceptor thermoelectric systems.	7
Figure 5. Molecular structures of several materials in this study. (a) meso-Tetra(4-carboxyphenyl)porphine (TCPP), (b) Chloro(protoporphyrinato)iron(III) (Hemin), (c) Protoporphyrin, (d) Zinc 2, 9, 16, 23-tetra-tert-butyl-29H, 31H-phthalocyanine (ZnPC), (e) cis-Bis(isothiocyanato)(2,2' -bipyridyl-4,4' -dicarboxylato)(4,4' -di-nonyl-2' -bipyridyl)ruthenium(II) (Z907), (f) Poly(3-hexylthiophene-2, 5-diyl) (P3HT), (g) [6, 6]-Phenyl C61 butyric acid methyl ester (PCBM)	8
Figure 6. Frontier orbital levels of P3HT, PCBM and the five dyes.	9
Figure 7. Chemical structures, UV-VIS, frontier orbitals, and absorption coefficients of TCPP, Hemin, and Protoporphyrin molecular units (MUs).	9
Figure 8. Schematic photoluminescence (PL) emission spectra of a pristine donor (D), a pristine acceptor (A), blend of the donor and the acceptor (D+A) in case of charge transfer (CT), and blend of the donor and the acceptor (D+A) in case of energy transfer (ET) [4].	11
Figure 9. Photoluminescence (PL) spectra of P3HT/Hemin in THF with Hemin concentration increase.	11
Figure 10. Photoluminescence (PL) spectra of P3HT/TCPP in THF with TCPP concentration increase.	12
Figure 11. Photoluminescence (PL) spectra of P3HT/Proto in THF with Proto concentration increase.	12
Figure 12. Stern-Volmer plots of the P3HT PL with Hemin, Protoporphyrin, and TCPP.	13
Figure 13. Frontier energy levels of all materials in fabricated solar cell devices.	13
Figure 14. Scheme of the solar cell device structure of P3HT/dye/PCBM fabricated in this study.	14
Figure 15. The J-V curves for P3HT/dye/PCBM solar cells.	15
Figure 16. The normalized trends of molar absorption coefficients (ϵ), PL quenching constants K_{sv} , LUMO orbital offsets $\Delta LUMO$ (δE), and the fabricated solar cell power conversion efficiencies (η) among three P3HT/dye pairs.	15
Figure 17. Correlation of K_{sv} versus $\Delta LUMO$ (δE) of P3HT/Dye.	16
Figure 18. (a) Synthetic scheme for hydroxyl terminated P3HT (b) Synthetic scheme for the P3HT-Hemin.	16
Figure 19. GPC traces of HO-P3HT-OH (blue line), Hemin (gray line), P3HT/hemin blend (yellow line) and P3HT-Hemin covalent system (red line).	17

Figure 20. UV-visible absorption spectra of P3HT (blue line), Hemin (yellow line), P3HT-Hemin covalent system (red line) and P3HT/Hemin blend (gray line) in THF. 18

Figure 21. PL of P3HT (blue line) and P3HT-Hemin (orange line) in 1×10^{-4} M THF. ... 19

Figure 22. The J-V curves of P3HT-Hemin/PCBM and P3HT/Hemin/PCBM solar cells. 20

Figure 23. Scheme of thermoelectric (Seebeck) process based on an n-type thermal doping: (a) before heating; (b) after heating and electron transfer or charge separation; (c) after electron transport or diffusion in the acceptor majority phase [4]. 21

Figure 24. Chemical structure of the four polymers studied. 22

Figure 25. Frontier orbital levels, energy gaps, and δE_2 values of the four polymers paired with iodine. 22

Figure 26. Scheme of electrical device and conductivity measurement set up. 23

Figure 27. IV curve of a 30% Iodine doped SF-PPV-2. 23

Figure 28. Correlation of electrical conductivity (σ) versus LUMO offset (δE_2) of polymer/Iodine pairs with Iodine doping levels at 15% (triangles) and 30% (squares)... 24

Table 1. Frontier orbital levels and absorption coefficients of P3HT, PCBM and five dyes (p8).

Table 2. Performance of ITO/PEDOT:PSS/P3HT:Dye:PCBM/Al Bulk heterojunction photovoltaic devices under a solar simulator (p14).

Table 3. GPC parameters of HO-P3HT-OH, P3HT-Hemin (p17).

Table 4. The photovoltaic parameters of P3HT/PCBM and P3HT/PCBM/Hemin. The calibrated PCE data are based on a reference standard solar cell RK5N3726 measured at the same set up and the same condition (p20).

Table 5. Correlation of conductivity versus LUMO offset of polymer/iodine pair (p24).

3. STATEMENT OF THE PROBLEMS STUDIED

Renewable, lightweight, mechanically flexible, and high efficiency power generation and energy conversion materials and devices (*e.g.*, converting light or heat into electrical power) has become a major scientific and technological challenge for the military due to widespread use of mobile electronic devices in modern battlefield. For instance, in a typical load of essential electronic devices each soldier is expected to carry in the battlefield, over 30% of the total load weights are due to the traditional chemical batteries in order to power the devices in a 24-hours period. For any flying objects in the air or space, lightweight, renewable, and flexible shaped power generating and converting systems are extremely critical.

3.1 Project Research Objectives

The immediate objective of this project research is to investigate a series of novel polymers and/or polymer/dye composite materials systems for potential high efficiency, lightweight, flexible, and portable photoelectric and thermoelectric power conversion devices. The long-term objectives of the project include elucidation of the fundamental mechanisms of photoelectric/thermoelectric processes in organic and polymeric materials.

3.2 Project Research Approaches

We will design, model, synthesize, process, and characterize a series of novel polymer/dye composite materials systems with frontier orbital levels (HOMOs and LUMOs) and morphologies systematically investigated and optimized for high efficiency photoelectric and thermoelectric energy conversion and radiation sensing applications. Specifically, the frontier orbital levels and energy gaps will be systematically investigated and optimized via molecular structural design and composite pairing among the conjugated polymer donors, dyes, acceptors, conductors, and electrodes, *etc.*, for instance, the polymer/dye pairing will be the first research task. The morphologies of the composite will also be optimized via chemical synthesis and solid state processing.

3.3 Project Challenges

The main technical challenge of the project is the availability of frontier orbital matched, stable, processable, and functionalizable conjugated polymers (both donor and acceptor types), dyes, and the development of polymer-dye covalently linked systems that could efficiently convert light/heat into electrical power. Therefore, frontier orbital matching studies and the materials design and chemical synthesis appear to be the most critical and challenging tasks.

4. SUMMARY OF MOST IMPORTANT RESULTS

4.1 Important Results On Photoelectric Studies

As described in the original project proposal, **Figure 1** illustrates a general frontier orbital (HOMOs/LUMOs) level scheme, and **Figure 2** exhibits a general free energy potential surface scheme of a typical donor/acceptor D/A binary organic/polymeric material system for high efficiency and cost effective optoelectronic energy conversion applications [1]. PI's previous modeling studies predicted that the photo generated excitation dissociation (or exciton quenching) at D/A interface occur most efficiently only at an intermediate or optimal LUMO offset (δE) of D/A pair as illustrated in **Figure 3**, *i.e.*, too small or too large δE would reduce the exciton dissociation [1-3]. As a matter of fact, one major research discovery from this project is that such theoretical prediction was indeed confirmed by some experimental data or results and will be elaborated in this report.

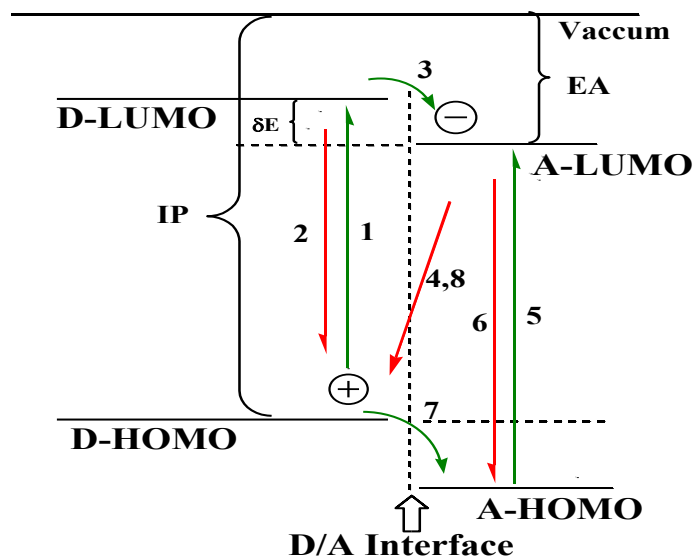


Figure 1. Scheme of molecular frontier orbitals and photo-induced charge transfer (CT) processes in an organic donor/acceptor binary light harvesting system.

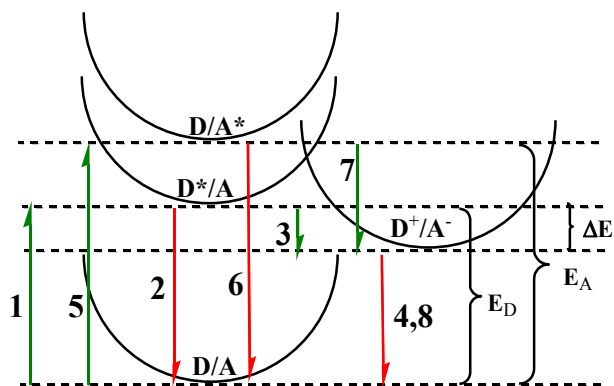


Figure 2. Scheme of standard Gibbs free-energy potential wells of photo-induced charge transfer processes in an organic donor/acceptor light harvesting system.

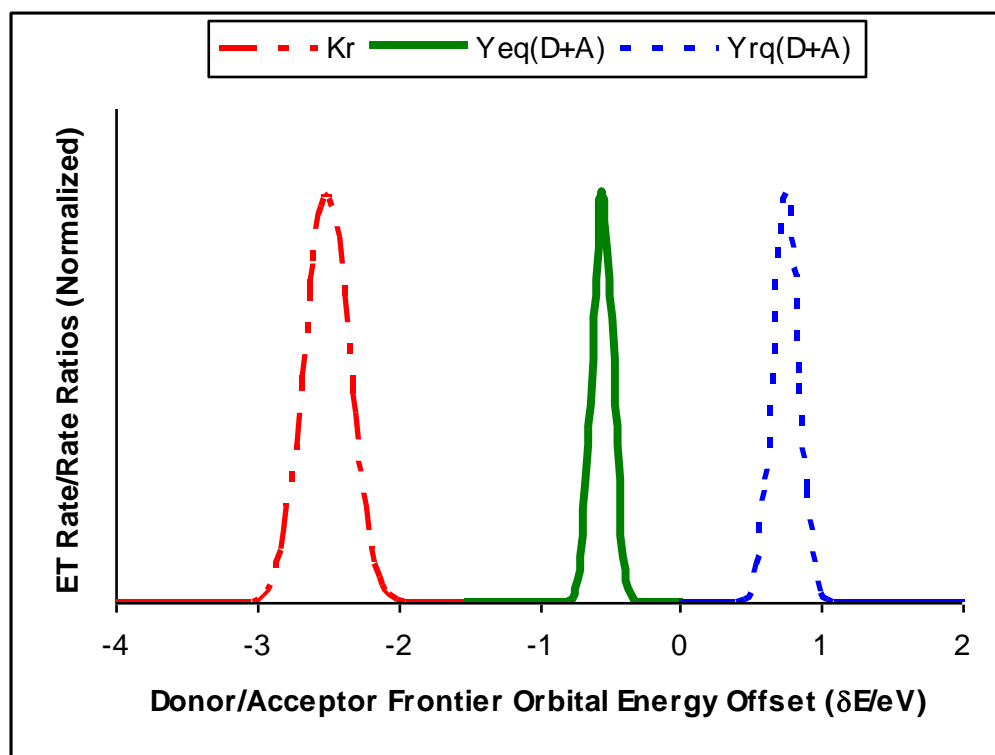


Figure 3. Scheme of photo induced exciton dissociation (or exciton quenching parameter, $Y_{eq(D+A)}$, middle solid curve), germinate charge recombination rate constant (K_r , left long dashed curve), and charge recombination quenching parameter ($Y_{rq(D+A)}$, right short dashed curve) versus LUMO offsets (ΔE) of a PPV based D/A pair [2-3].

The proposed project research include two thrust areas: 1) A polymer/dye/acceptor three-component photoelectric conversion system as shown in **Figure 4a**, and 2) A strong D/A pair with weakly coupled organic system for thermoelectric conversion system as shown in **Figure 4b**.

The polymer/dye/acceptor three-component system has two potential advantages compared to the common donor/acceptor binary system: 1) it minimizes the photo or thermally generated electron-hole pair recombination due to electrons and holes are moving away from each other via an intermediate molecular unit (MU, such as a molecular dye), and 2) availability of a vast variety of molecular dyes or units with different frontier orbitals, energy gaps, and radiation absorption coefficients that may match well with the intended radiation photons.

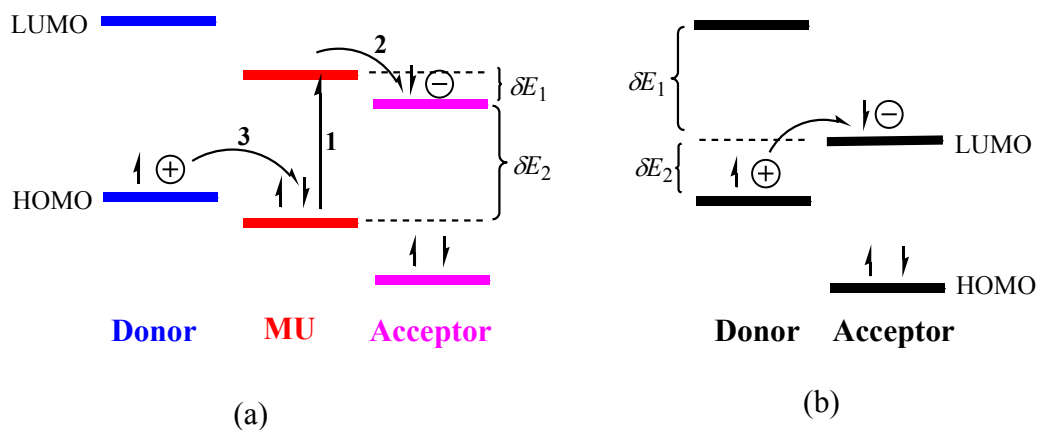


Figure 4. Frontier orbital schemes of (a) proposed dye molecular units (MUs) sensitized triple-component organic photoelectric systems and (b) organic donor/acceptor thermoelectric systems.

During the project period, we systematically evaluated optoelectronic properties of a series of polymers, dyes, and their composites, with particular focus on four dyes, one polymer, and one acceptor: (a) meso-Tetra(4-carboxyphenyl)porphine (TCPP), (b) Chloro(protoporphyrinato)iron(III) (Hemin), (c) Protoporphyrin (Proto), (d) Zinc 2, 9, 16, 23-tetra-tert-butyl-29H, 31H-phthalocyanine (ZnPC), (e) cis-Bis(isothiocyanato)(2,2'-bipyridyl-4,4'-dicarboxylato)(4,4'-di-nonyl-2'-bipyridyl)ruthenium(II) (Z907), (f) Poly(3-hexylthiophene-2, 5-diyl) (P3HT), (g) [6, 6]-Phenyl C61 butyric acid methyl ester (PCBM), where the chemical structures of these materials are shown in **Figure 5**. The measured frontier orbitals (via CV and UV-Vis) of these materials are shown in **Figure 6**. **Table 1** lists the data of frontier orbitals, energy gaps, and optical absorption molar extinction coefficients. It appears that the frontier orbital levels would make ZnPc and Z907 dyes as energy transfer acceptor units in reference to P3HT, and three dyes Hemin, TCPP, and Proto exhibit electron acceptor type frontier orbitals compared to P3HT, and exhibit electron donor type frontier orbitals compared to PCBM, *i.e.*, these three dyes appear to be the desired middle molecular units (MUs) or ideal candidates for investigating the proposed three-component optoelectronic system. The UV-Vis absorption spectra were illustrated in **Figure 7**.

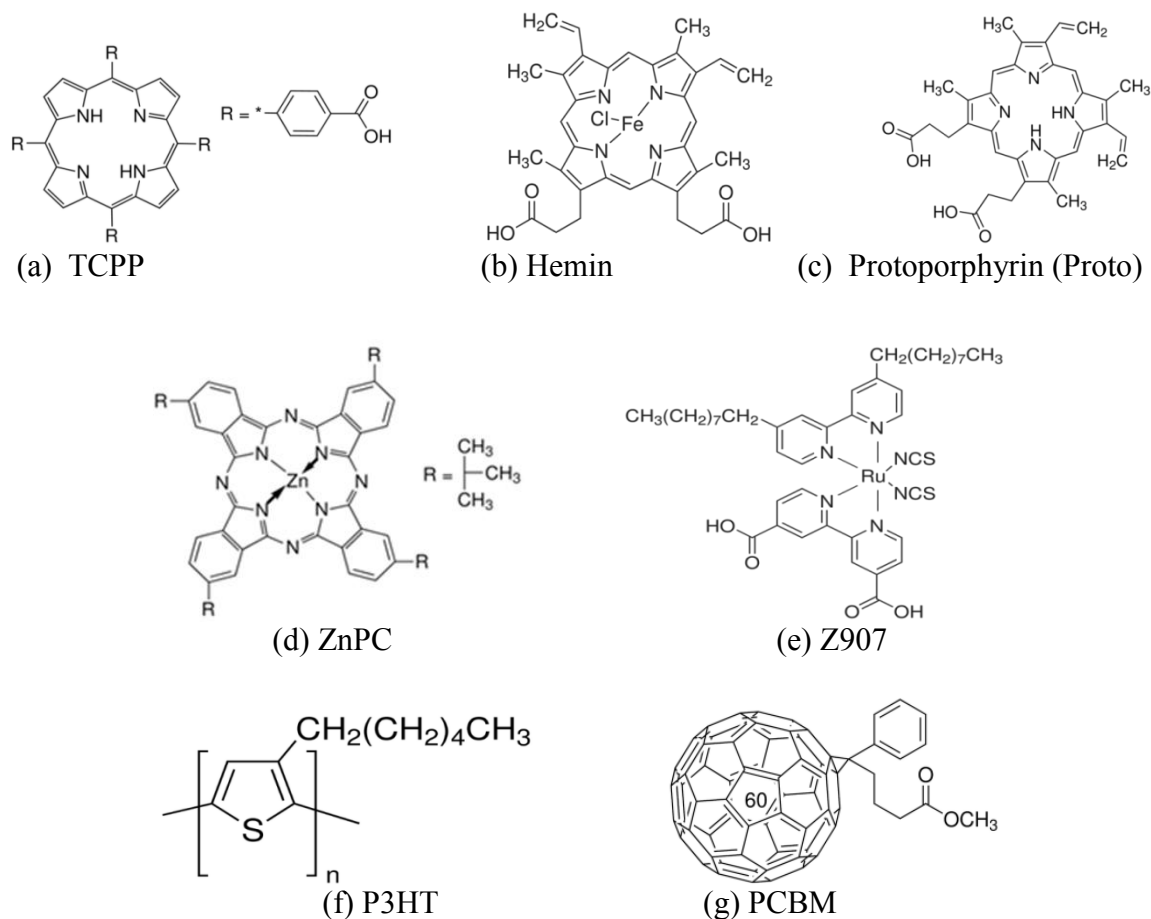


Figure 5. Molecular structures of several materials in this study. (a) meso-Tetra(4-carboxyphenyl)porphine (TCPP), (b) Chloro(protoporphyrinato)iron(III) (Hemin), (c) Protoporphyrin, (d) Zinc 2, 9, 16, 23-tetra-tert-butyl-29H, 31H-phthalocyanine (ZnPC), (e) cis-Bis(isothiocyanato)(2,2'-bipyridyl-4,4'-dicarboxylato)(4,4'-di-nonyl-2'-bipyridyl)ruthenium(II) (Z907), (f) Poly(3-hexylthiophene-2, 5-diyl) (P3HT), (g) [6, 6]-Phenyl C61 butyric acid methyl ester (PCBM)

Table 1. Frontier orbital levels and absorption coefficients of P3HT, PCBM and five dyes.

	P3HT(s)	TCPP	Proto	Hemin	ZnPC	Z907	PCBM
HOMO,eV	-5.05	-5.45	-5.13	-5.33	-4.83	-4.92	-6.18
LUMO,eV	-2.73	-3.57	-3.19	-3.49	-3.03	-2.97	-3.82
Eg,eV	2.32	1.88	1.94	1.84	1.80	1.95	2.36
Molar Absorption Coefficient ($M^{-1}cm^{-1}$)	1.2×10^4	1.39×10^5	1.05×10^5	3.08×10^4	2.02×10^5	3.91×10^3	4.82×10^4

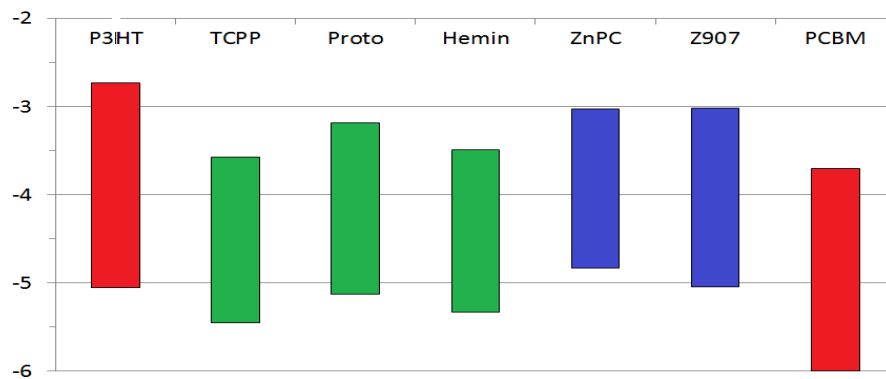


Figure 6. Frontier orbital levels of P3HT, PCBM and the five dyes.

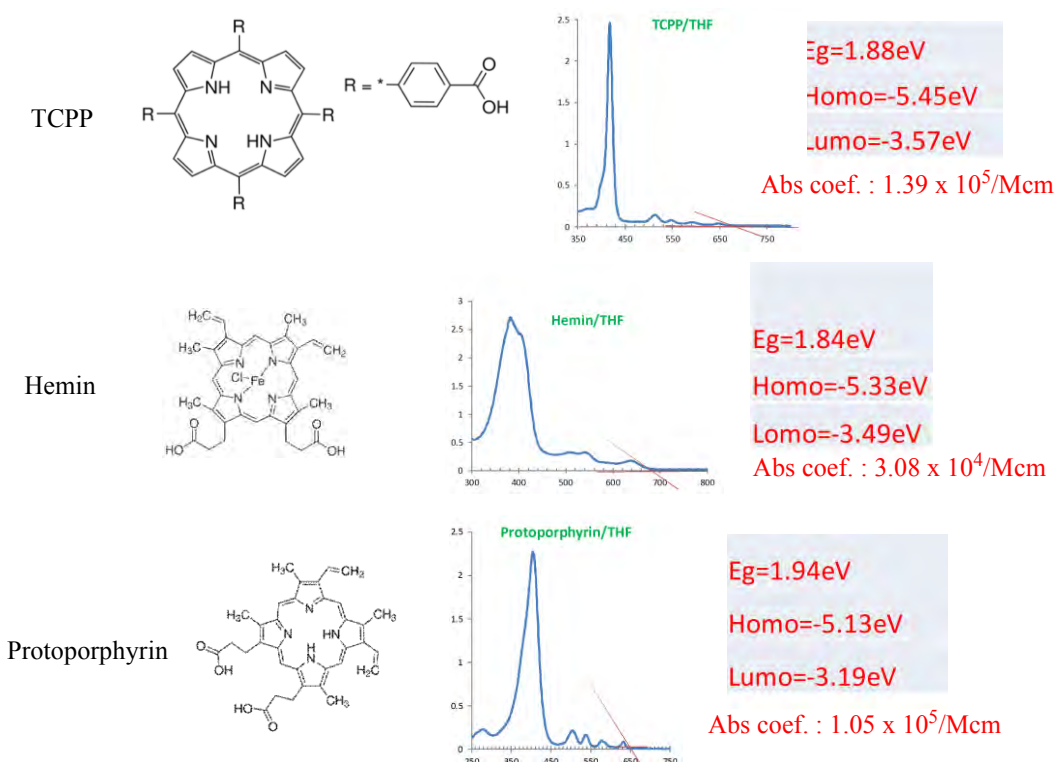


Figure 7. Chemical structures, UV-VIS, frontier orbitals, and absorption coefficients of TCPP, Hemin, and Protoporphyrin molecular units (MUs).

Charge Transfer (CT) and Energy Transfer (ET) Studies

The charge transfer (CT) and/or energy transfer (ET) in a D/A pair can be experimentally determined via photoluminescence (PL) measurements if donor and acceptor exhibit PL emissions. For instance, as schematically illustrated in **Figure 8** [4], assuming a hypothetical pristine donor (exciton/energy or charge donor) exhibits a normalized PL emission peak at 500 nm (2.48 eV), and a hypothetical pristine acceptor (exciton/energy or charge acceptor) exhibits a normalized PL emission peak at 600 nm (2.07 eV), and both have the same quantity. In the case where photo induced charge

transfer (CT) occurs between the pair, the PL emissions of both should be quenched by a same quanta corresponding to the number of transferred charges (designated as ΔPL_{CT} that can be measured/estimated directly from the PL emission peak changes), for instance, by a hypothetical $\Delta PL_{CT} = 50\%$ PL peak decrease of D+A (CT) curve in Figure 3.40. In the case where photo induced energy or exciton transfer proceeds from the donor to the acceptor, then the donor PL should be decreased by the same quanta (designated as ΔPL_{ET}) while the acceptor PL should be increased by the same amount, for instance, by a hypothetical $\Delta PL_{ET} = 30\%$ in D+A (ET) as shown in **Figure 8** [4].

Suppose both CT and ET may occur simultaneously in a D+A blend, *i.e.*, in a hypothetic case of D+A (CT+ET). Using ΔPL_D as the total PL emission peak change of D, ΔPL_A as the total PL emission peak change of A, ΔPL_{DD} represents the donor PL emission peak change due to the D concentration change, ΔPL_{DA} represents the donor PL emission peak change due to the A concentration change, ΔPL_{AD} represents the acceptor PL emission peak change due to the D concentration change, ΔPL_{AA} represents the acceptor PL emission peak change due to the A concentration change, and assuming other factors such as aggregation induced PL quenching can be neglected in very dilute solution, the following relationships or approximations may apply

$$\Delta PL_D = \Delta PL_{CT} + \Delta PL_{ET} + \Delta PL_{DD} + \Delta PL_{DA} \quad (1)$$

$$\Delta PL_A = \Delta PL_{CT} - \Delta PL_{ET} + \Delta PL_{AA} + \Delta PL_{AD} \quad (2)$$

Combining equations 1 and 2, one obtains

$$\Delta PL_{CT} = (\Delta PL_D + \Delta PL_A - \Delta PL_{DD} - \Delta PL_{DA} - \Delta PL_{AA} - \Delta PL_{AD})/2 \quad (3)$$

Equation 3 provides an estimate of charge transfer (CT) contribution if both CT and ET occurs in a D/A pair and both exhibit PL [4].

In our studies, the D (P3HT) concentration is fixed, ΔPL_{DD} and ΔPL_{AD} become zero. Also, the dye emission do not contribute to P3HT peak emission (other than CT and ET), the ΔPL_{DA} can also be neglected. So equation (3) becomes

$$\Delta PL_{CT} = (\Delta PL_D + \Delta PL_A - \Delta PL_{AA})/2 \quad (4)$$

Equation (4) is being applied in our studies to estimate charge transfer (CT) component of the P3HT/Dye PL quenching data. For instance, at 440nm excitation wavelength, Proto exhibits about 100% CT without ET, while TCPP exhibits about 40% ET and 60% CT [5]. To our knowledge, this is the first attempt or approach to distinguish the fraction of CT versus ET when both occurs in one D/A pair.

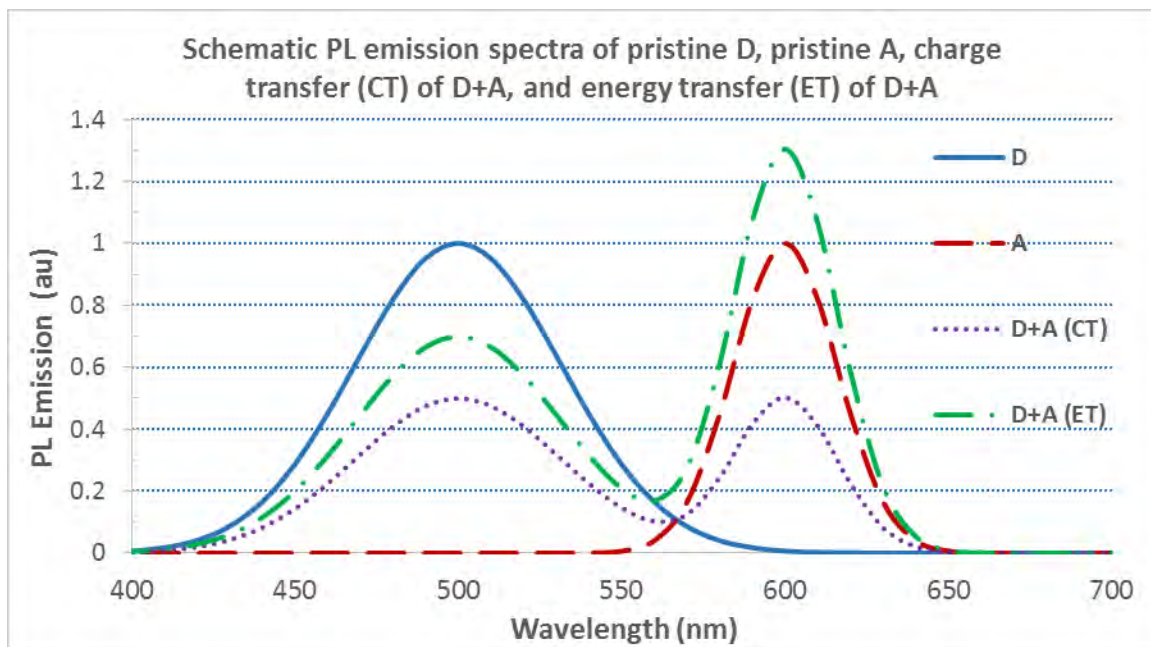


Figure 8. Schematic photoluminescence (PL) emission spectra of a pristine donor (D), a pristine acceptor (A), blend of the donor and the acceptor (D+A) in case of charge transfer (CT), and blend of the donor and the acceptor (D+A) in case of energy transfer (ET) [4].

The dye concentration dependent PL quenching spectra of P3HT with each dyes are shown in **Figures 9, 10** and **11**, where the PL data (ΔPL_D and ΔPL_A) are combined with pure dye PL data (ΔPL_{AA}) obtained separately, so the charge transfer CT component can be calculated from equation (4). The Stern-Volmer (SV) PL quenching plots based on CT are plotted and shown in **Figure 12**. It can be seen that CT induced PL quenching coefficients (K_{sv}) follows a descending order from Hemin, Protoporphyrin, to TCPP.

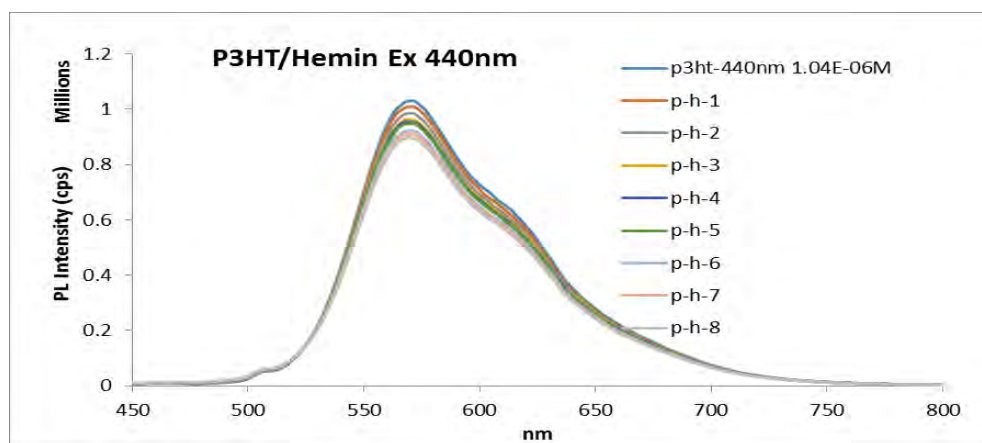


Figure 9. Photoluminescence (PL) spectra of P3HT/Hemin in THF with Hemin concentration increase.

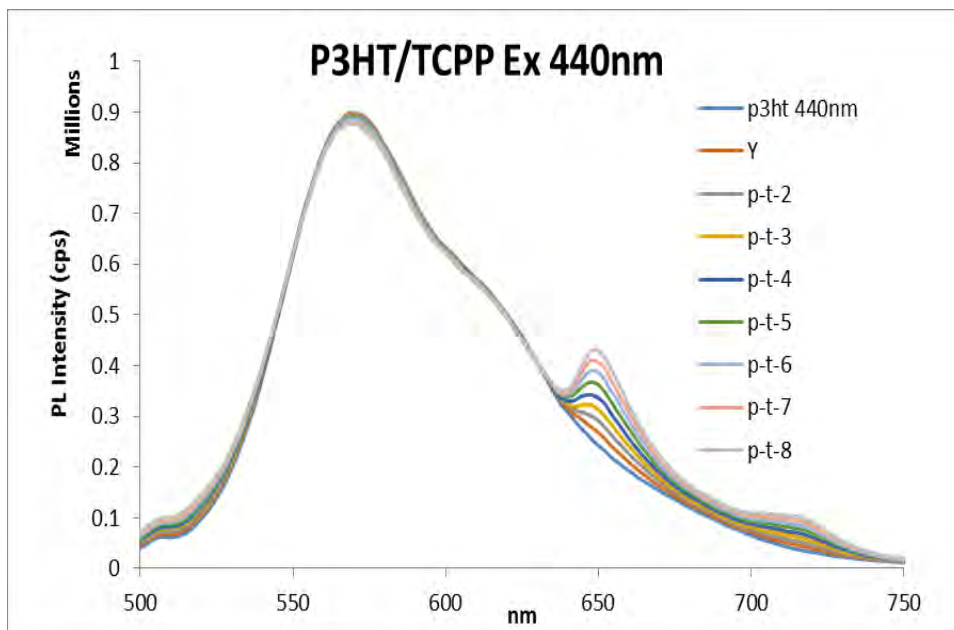


Figure 10. Photoluminescence (PL) spectra of P3HT/TCPP in THF with TCPP concentration increase.

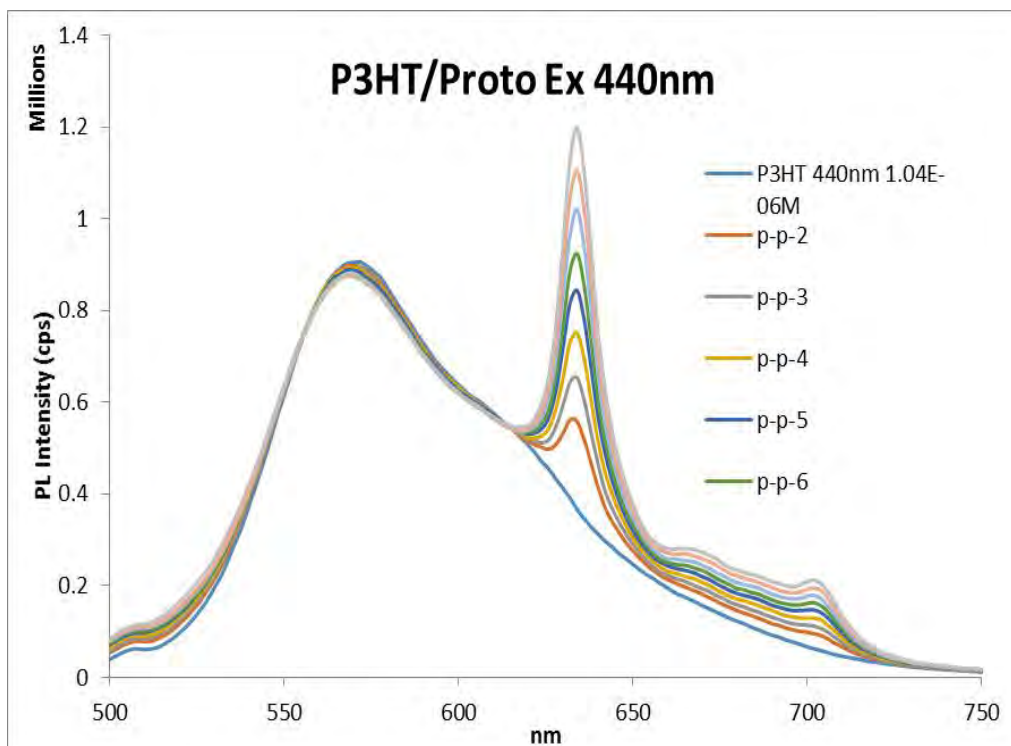


Figure 11. Photoluminescence (PL) spectra of P3HT/Proto in THF with Proto concentration increase.

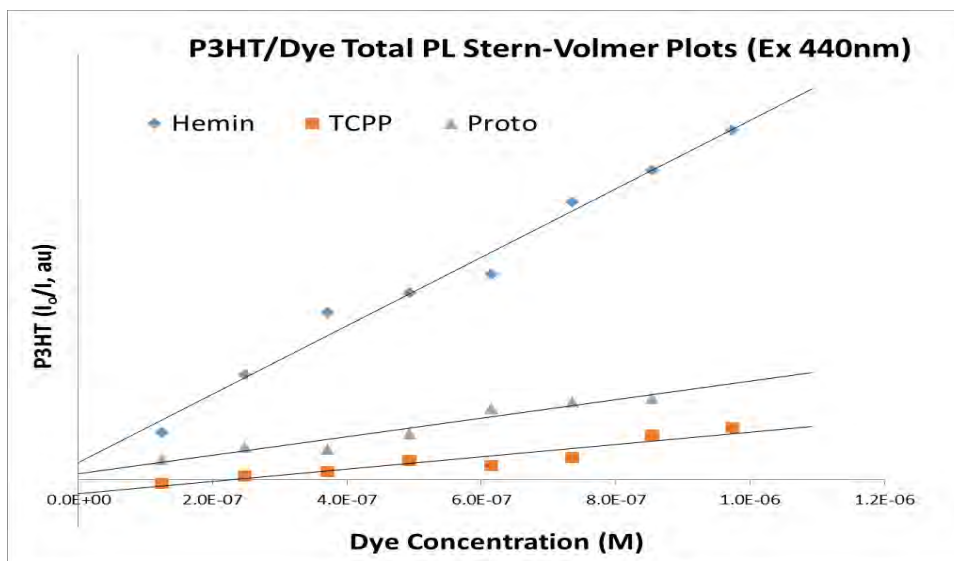


Figure 12. Stern-Volmer plots of the P3HT PL with Hemin, Protoporphyrin, and TCPP.

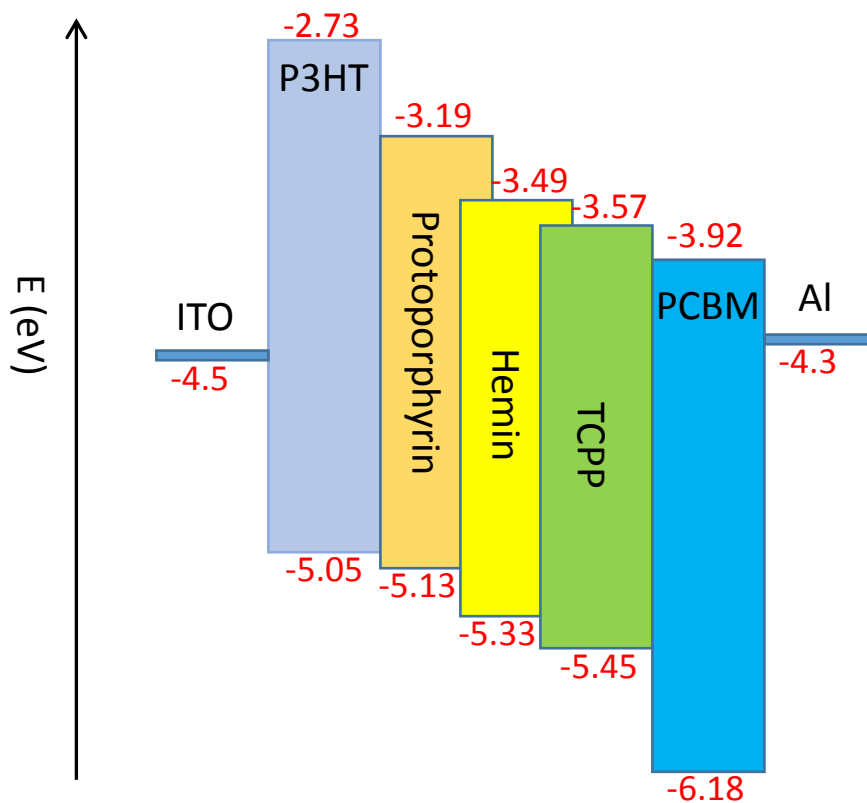


Figure 13. Frontier energy levels of all materials in fabricated solar cell devices.

In preliminarily fabricated and tested (but not yet optimized) solar cells made of the P3HT/dye/PCBM composites (cell frontier orbital levels and structural schemes are shown in **Figure 13** and **14**), the short circuit current densities J_{sc} as well as the overall

power conversion efficiencies (PCE) also follow a descending order from Hemin, Protoporphyrin, to TCPP (**Figure 15** and **Table 2**), despite Hemin has the smallest absorption coefficient (ϵ). **Figure 16** exhibits comparisons of absorption coefficients (ϵ), dye/P3HT PL quenching constants (K_{sv}), dye/P3HT LUMO offsets (δE), and power conversion efficiencies (η) of three solar cells fabricated from the P3HT/dye/PCBM composites. Most notably, the power conversion efficiencies of the solar cells follows the PL quenching trend nicely, *i.e.*, the Hemin dye with strongest PL quenching to P3HT exhibits best power conversion efficiency. However, as exhibited in **Figure 17** and **Table 1**, the Hemin dye exhibits an intermediate polymer-dye LUMO offset (δE) and lowest absorption coefficient (ϵ) as compared to the other two dyes. This reveals two critical information: 1) Too much LUMO offset or electron transfer driving force results in smaller PL quenching and smaller power conversion efficiency, this could be another critical experimental evidence for the Marcus “inverted” electron transfer model; 2) Optimum electron transfer driving force or strong PL quenching appears much more critical than absorption coefficient for optoelectronic conversion coefficients. This study shall be continued with more molecular light harvesting units or dyes to further verify such key observation or conclusion.

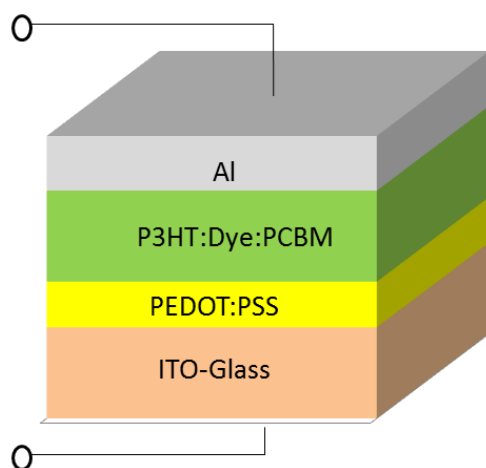


Figure 14. Scheme of the solar cell device structure of P3HT/dye/PCBM fabricated in this study.

Table 2. Performance of ITO/PEDOT:PSS/P3HT:Dye:PCBM/Al Bulk heterojunction photovoltaic devices under a solar simulator.

	J_{sc} (mA/cm ²)	V_{oc} (Volt)	FF (%)	PCE (% un-calibrated)
Hemin	4.1	0.24	25.624	0.25
Proto	1.07141	0.16	22.615	0.038
TCPP	0.73412	0.28	15.723	0.033

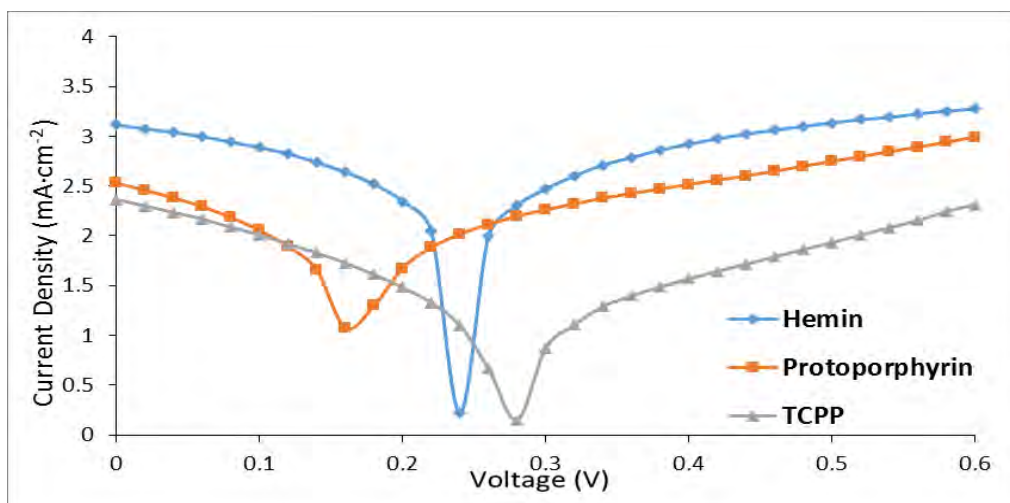


Figure 15. The J-V curves for P3HT/dye/PCBM solar cells.

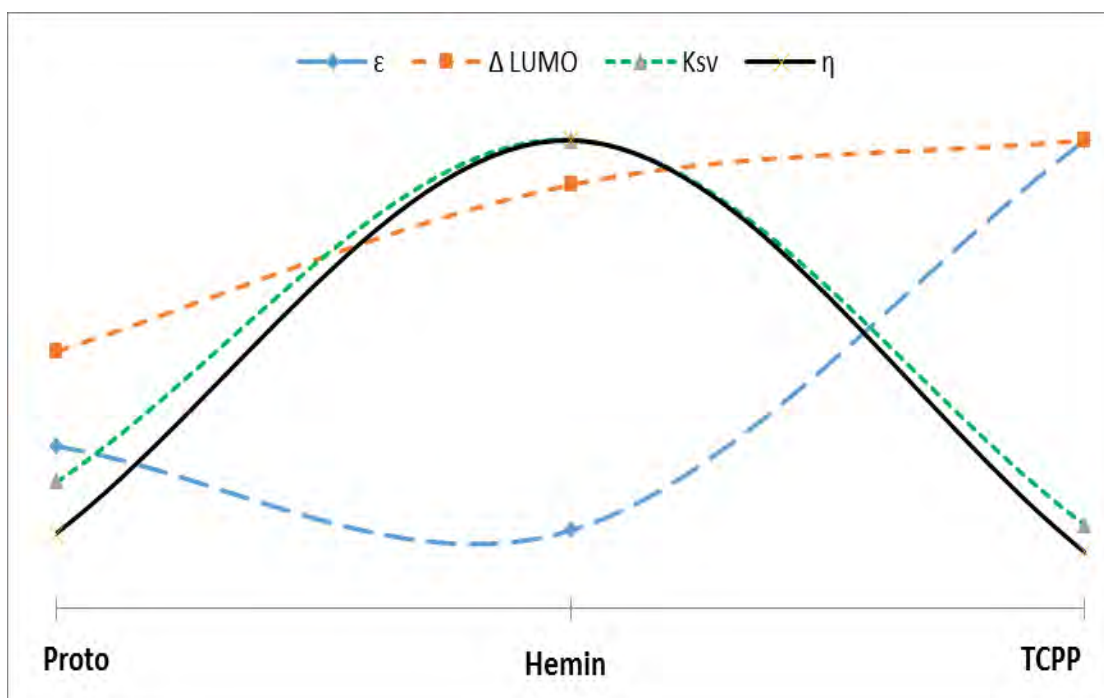


Figure 16. The normalized trends of molar absorption coefficients (ϵ), PL quenching constants K_{sv} , LUMO orbital offsets $\Delta LUMO$ (δE), and the fabricated solar cell power conversion efficiencies (η) among three P3HT/dye pairs.

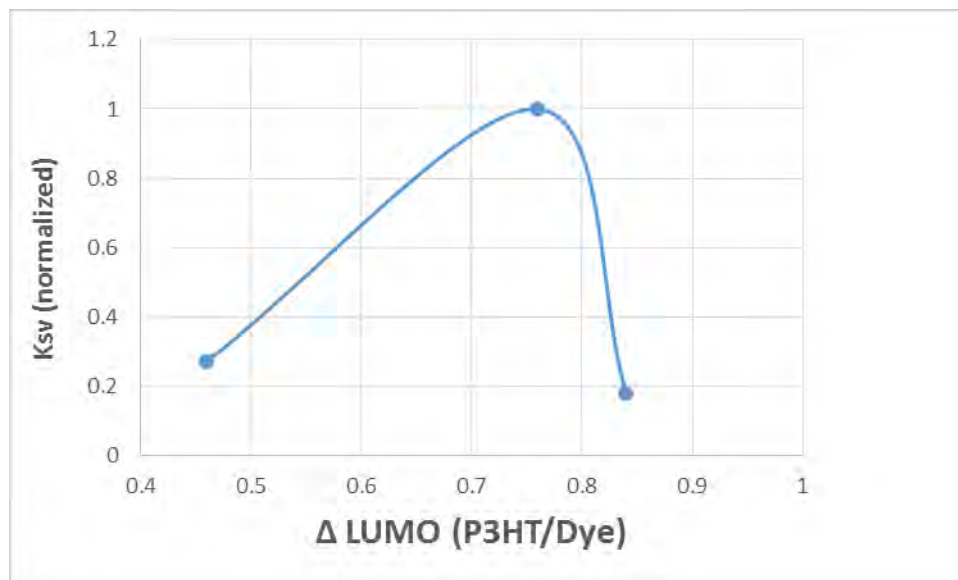


Figure 17. Correlation of K_{sv} versus $\Delta LUMO$ (δE) of P3HT/Dye.

Synthesis and Characterization of a Covalent P3HT-Hemin System.

Another major accomplishment is the covalent coupling of Hemin dye to the two ends of the P3HT, where the synthetic scheme is shown in **Figure 18**.

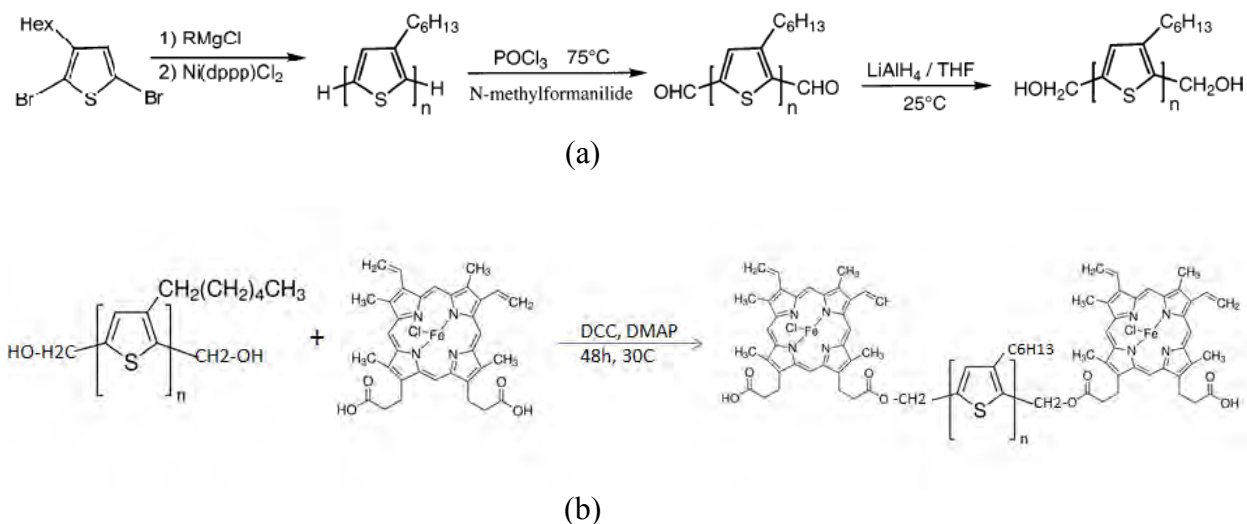


Figure 18. (a) Synthetic scheme for hydroxyl terminated P3HT (b) Synthetic scheme for the P3HT-Hemin

The covalent P3HT-Hemin is prepared in four steps as shown in **Figure 18a-b**: (1) Synthesis of Poly(3-hexylthiophene) with H/H End Group, (2) Synthesis of Poly(3-hexylthiophene) with CHO/CHO End Group, (3) Synthesis of Poly(3-hexylthiophene) with HO/HO End Group and (4) synthesis of P3HT-Hemin.

The formation of H/H terminated Poly(3-hexylthiophene) was characterized by proton NMR, where the proton peak integration revealed the synthesized P3HT has about 49 repeat units. The final formation of P3HT-Hemin polymer-dye complexes were also characterized by gel permeation chromatography (GPC) (**Figure 19** and **Table 3**). P3HT synthesized in this study has a narrow molecular weight distribution ($M_n=8400$, $M_w/M_n=1.15$). After the two ends hydroxyl terminated P3HT was reacted with Hemin ($M_n=652\text{g/mol}$), the GPC traces shifted to higher molecular weights ($M_n=9638$), indicating that the two Hemin dyes ($2 \times 652 = 1304$) were attached to both sides of P3HT chain (**Table 3**).

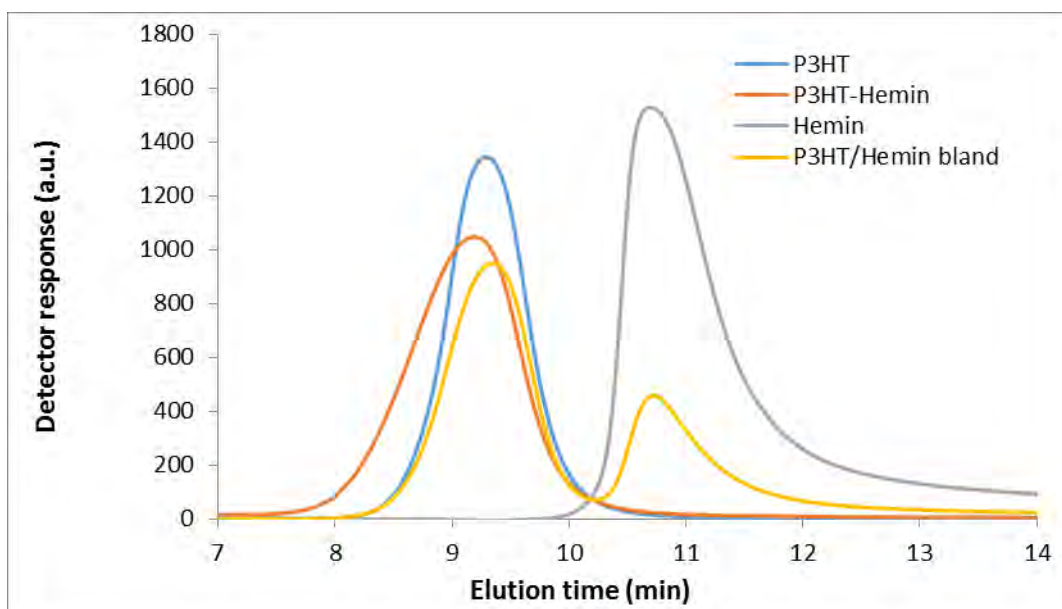


Figure 19. GPC traces of HO-P3HT-OH (blue line), Hemin (gray line), P3HT/hemin blend (yellow line) and P3HT-Hemin covalent system (red line).

Table 3. GPC parameters of HO-P3HT-OH, P3HT-Hemin.

	HO-P3HT-OH	P3HT-Hemin
Mn - (Daltons)	8430	9638
Mw - (Daltons)	9666	11012
Mz - (Daltons)	10860	12345
Mp - (Daltons)	9398	10663

Figure 20 shows the UV-visible absorption spectra of P3HT (blue line), Hemin (purple line), P3HT-Hemin (red line) and P3HT/Hemin blend (green line) in THF solution. The maximum absorption wavelength (λ_{max}) of covalent P3HT-Hemin at 419nm was blue shifted comparing to pure P3HT with λ_{max} at 445nm, and also different with the absorption spectra of P3HT/Hemin blend or pure Hemin. It also implies that covalent P3HT-Hemin was synthesized successfully.

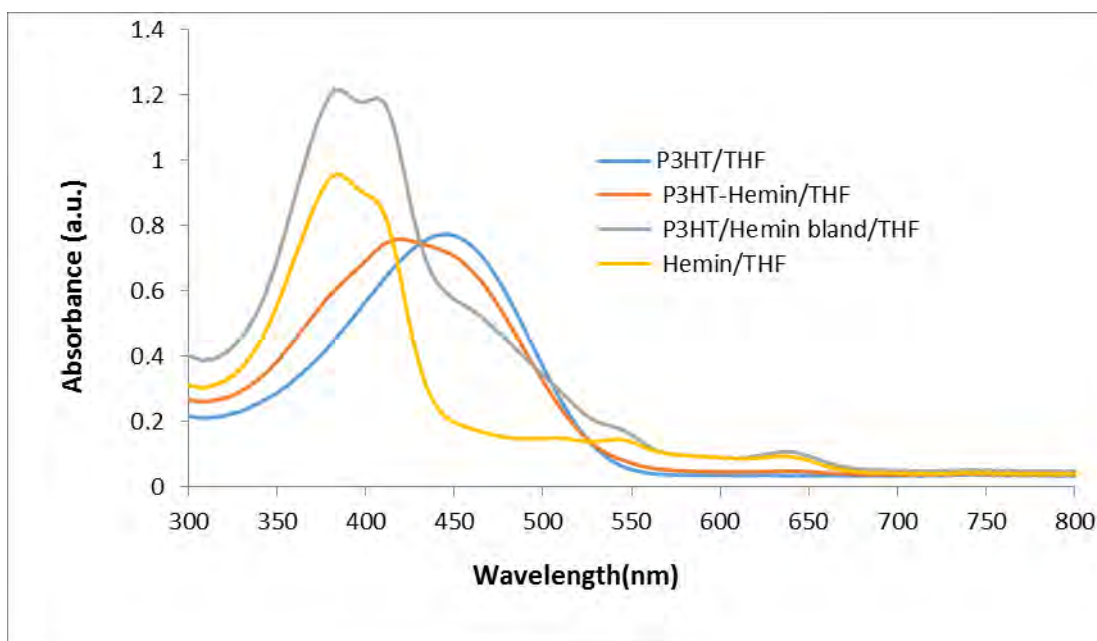


Figure 20. UV-visible absorption spectra of P3HT (blue line), Hemin (yellow line), P3HT-Hemin covalent system (red line) and P3HT/Hemin blend (gray line) in THF.

Another evidence for the formation of P3HT-Hemin is the photoluminescence (PL) quenching comparison of pure P3HT and P3HT-Hemin in THF solution as shown in **Figure 21**. Different excitation wavelengths (400nm and 375nm) were used to excite P3HT and P3HT-Hemin with the same P3HT concentration (1.0×10^{-4} M). The PL peaks of P3HT and P3HT-Hemin are almost same at 470nm and 468nm, respectively, while the PL peak of P3HT-Hemin sample exhibited more about 60% quenching compared to pure P3HT solution. The PL quenching can be attributed to photo induced charge transfer (CT) from P3HT to Hemin in P3HT-Hemin chain.

Finally, an AM 1.5G solar simulator was used to study the efficiency of the fabricated solar cell devices, where the photo JV curves of the cells are shown in **Figure 22**, and the open circuit voltage (V_{oc}), short circuit current (J_{sc}), fill factor (FF), power conversion efficiency (η , un-calibrated and calibrated) data are listed in **Table 4**. The calibrated PCE data are based on a reference standard Silicon solar cell RK5N3726 (from ABET Technologies) measured at the same set up and the same condition.

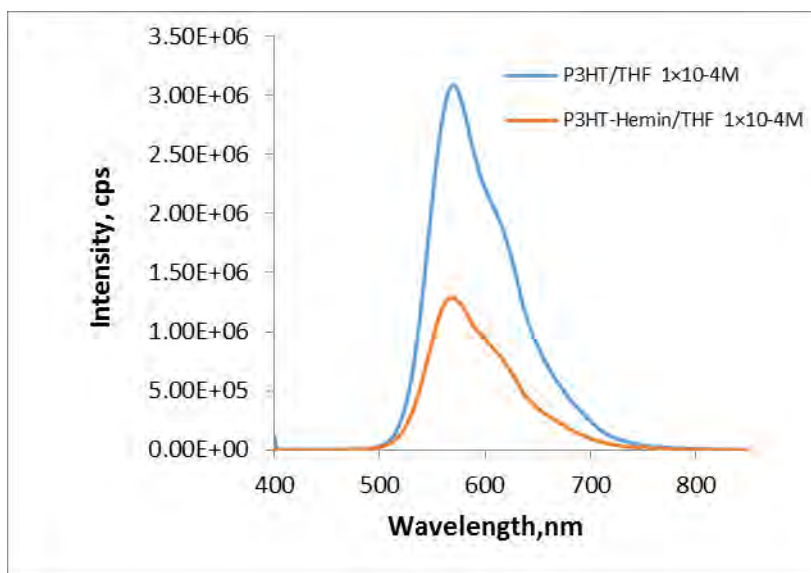


Figure 21. PL of P3HT (blue line) and P3HT-Hemin (orange line) in 1×10^{-4} M THF.

The results indicate that P3HT-Hemin/PCBM solar cell devices exhibits a 63% enhancement of PCE, 9.8% enhancement of J_{sc} , and 28.6% enhancement of V_{oc} than P3HT/Hemin/PCBM blend cells, and 16% enhancement of V_{oc} than P3HT/PCBM cells. Better photo induced charge separation appears to be the key factor in P3HT-Hemin/PCBM cells due to more convenient reach of photo generated excitons toward the P3HT-Dye interface.

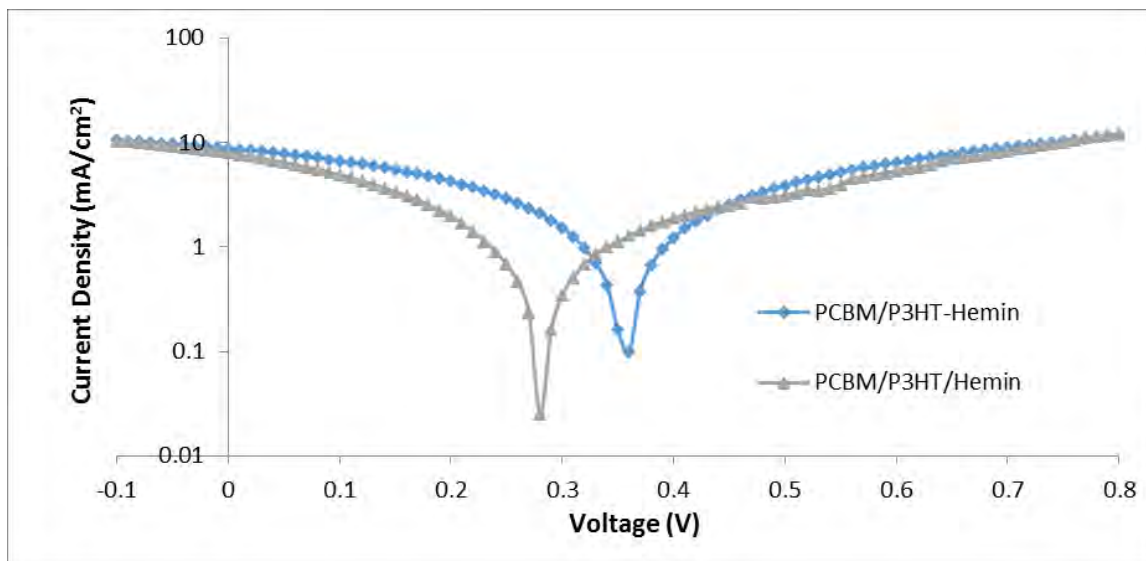


Figure 22. The J-V curves of P3HT-Hemin/PCBM and P3HT/Hemin/PCBM solar cells.

Table 4. The photovoltaic parameters of P3HT/PCBM and P3HT/PCBM/Hemin. The calibrated PCE data are based on a reference standard solar cell RK5N3726 measured at the same set up and the same condition.

	P3HT-Hemin/PCBM	P3HT/PCBM/Hemin
Jsc, mA/cm ²	8.74	7.96
Voc, V	0.36	0.28
FF, %	27.14	23.17
PCE, %	0.86	0.53
PCE, % (Calibrated)	3.18	1.95

Future work include a systematic screening of more polymer/dye pairs with more severe PL quenching (an intermediate optimal Δ LUMO need to be identified), and better solid state morphologies, and to further optimize the processing and fabricating conditions of polymer/dye optoelectronic devices.

4.2 Important Results On Thermoelectric Studies

In a strong donor/acceptor pair where the donor HOMO is close but slightly lower than the LUMO of an acceptor as shown in **Figure 4b** and **Figure 23** [4], once the electron is transferred from the D-HOMO to the A-LUMO as a result of heat or ΔT , it can move away from the donor dopant site (*i.e.*, donor is the minority) in the acceptor LUMO band (*i.e.*, acceptor is the majority, **Figure 23b**) due to both mobile electron density or chemical potential gradient or a temperature gradient ΔT . Such electron transport or migration in the material would result a spatial voltage ΔV as shown in **Figure 23c**. The thermoelectric Seebeck coefficient (S), the thermal power factor (TPF), and a figure of merit (ZT) of thermal electric materials are defined as

$$S = \Delta V / \Delta T \quad (5)$$

$$\text{TPF} = S^2 \sigma \quad (6)$$

$$\text{ZT} = S^2 \sigma T / \kappa \quad (7)$$

Where σ is the electrical conductivity, and κ is the thermal conductivity. Clearly, in order to increase the Seebeck coefficient and other thermoelectric properties, it is crucial to 1) increase thermal doping generated charge carrier density which contribute to both ΔV and σ , and 2) improve electron transport or the acceptor LUMO bandwidth E_w that also contribute to both ΔV and σ . Thermal doping generated electron density is proportional to the thermal incurred electron transfer rate which in turn are related to the driving forces such as kT (due to ΔT) and the counter driving forces such as δE_2 and a charge transfer reorganization energy λ (**Figure 4b**). Based on Marcus electron transfer model, an optimal thermo-doping charge generation condition appears to be when

$$kT - \delta E_2 - \lambda = 0 \quad (8)$$

i.e., there could exist an optimal δE_2 at specific kT and λ values.

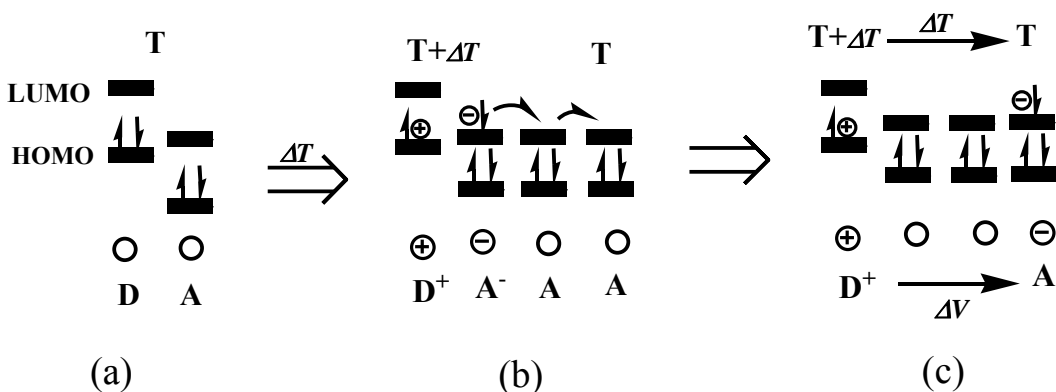


Figure 23. Scheme of thermoelectric (Seebeck) process based on an n-type thermal doping: (a) before heating; (b) after heating and electron transfer or charge separation; (c) after electron transport or diffusion in the acceptor majority phase [4].

In order to investigate the correlation of thermo-doping generated charge carrier density (or conductivity σ) versus δE_2 as discussed above, a series of D type polymers with differing δE_2 values of a D/A pair need to be synthesized and studied. In this work, four PPV type polymers have been successfully synthesized (chemical structures are shown in **Figure 24**), and their frontier frontier orbital levels, energy gaps, and the δE_2 values with a strong acceptor Iodine are shown in **Figure 25**. The four synthesized PPVs appear ideal for the σ - δE_2 correlation studies due to their gradual decreasing of HOMO levels, and that the charge transfer reorganization energy (λ) should be similar due to similar chemical structures. **Figure 26** exhibits a simple device and conductivity measurement scheme, and **Figure 27** exhibits an example IV curve of a 30% doped SF-

PPV2 film. **Table 5** lists the 30% Iodine doped conductivity data of the four polymers versus their δE_2 values, and **Figure 28** exhibits the conductivity versus both 30% and 15% Iodine doped polymers.

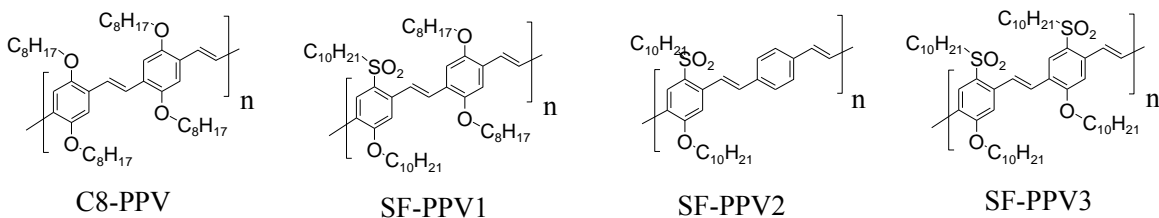


Figure 24. Chemical structure of the four polymers studied.

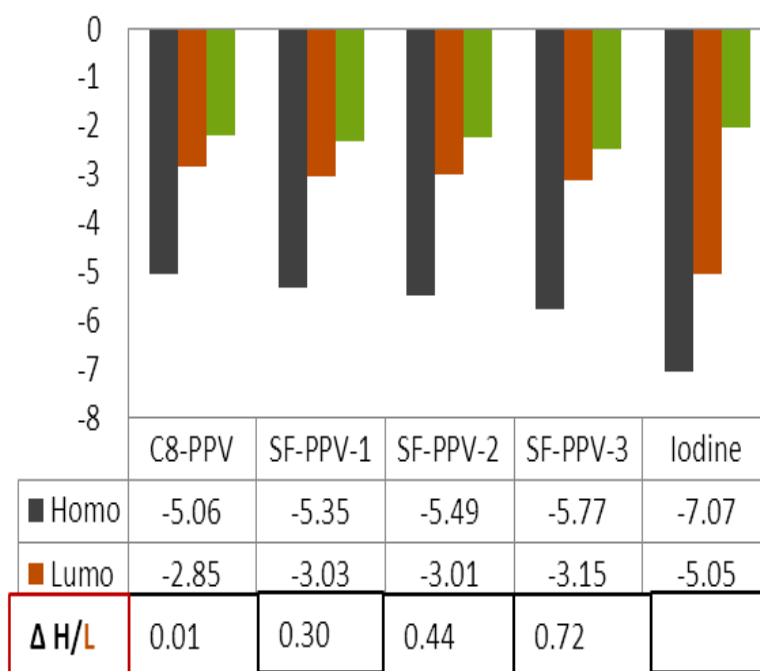


Figure 25. Frontier orbital levels, energy gaps, and δE_2 values of the four polymers paired with iodine.

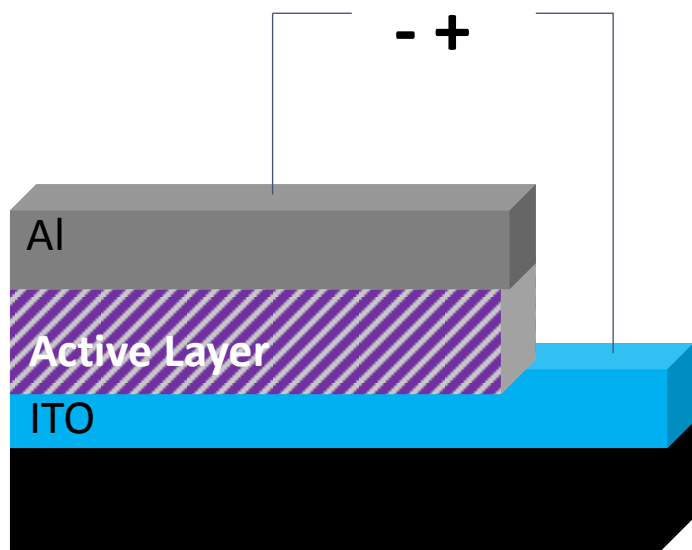


Figure 26. Scheme of electrical device and conductivity measurement set up.

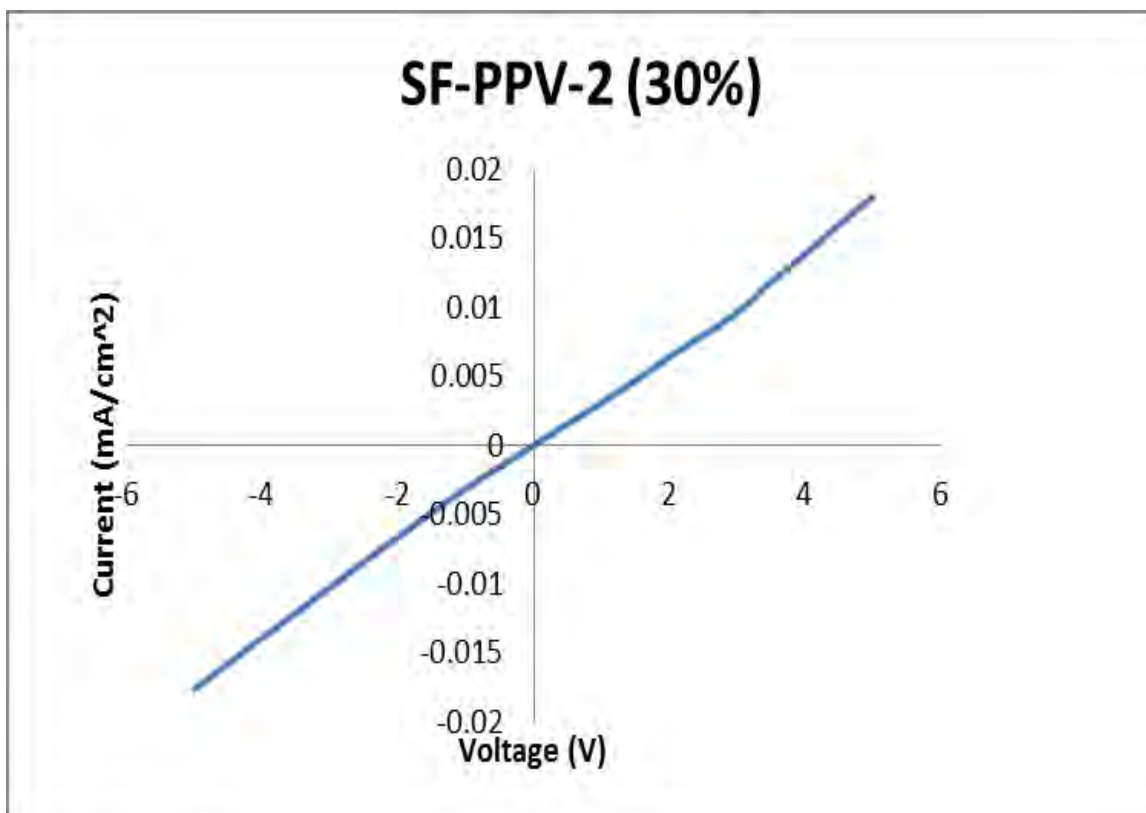
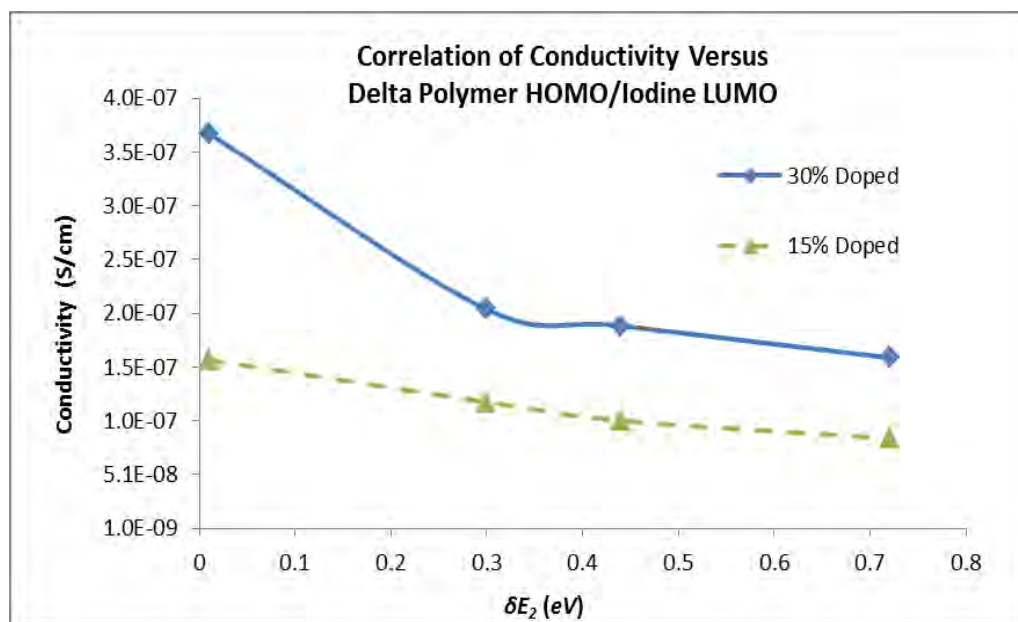


Figure 27. IV curve of a 30% Iodine doped SF-PPV-2.

Table 5. Correlation of conductivity versus LUMO offset of polymer/iodine pair.

Polymer name	δE	σ (S/cm, 30% doped)	σ (S/cm, 15% doped)
C8-PPV	0.01	3.68×10^{-7}	2.06×10^{-7}
SF-PPV-1	0.30	2.05×10^{-7}	1.17×10^{-7}
SF-PPV-2	0.04	1.90×10^{-7}	9.25×10^{-8}
SF-PPV-3	0.72	1.60×10^{-7}	3.30×10^{-8}

**Figure 28.** Correlation of electrical conductivity (σ) versus LUMO offset (δE_2) of polymer/Iodine pairs with Iodine doping levels at 15% (triangles) and 30% (squares).

Based on data from **Figure 28**, it appears the conductivity (or room temperature thermal doped charge carrier density) are decreasing as δE_2 increases for this particular set of PPVs. This implies, the key thermal doping driving force at room temperature is smaller than the two counter-driving forces (*i.e.*, $kT < \delta E_2 + \lambda$), so the system is in the normal region of Marcus electron transfer model [2-3, 6-7]. One key next step research include decreasing the δE_2 (or increasing the kT) to find out if an optical condition exist for most efficient thermoelectric charge generation.

In summary, this research revealed several important or critical information: 1) Too much LUMO offset or electron transfer driving force between the polymer and dye
 Norfolk State University/Sun

would result in weaker PL quenching and optoelectronic device power conversion efficiency, this experimentally confirmed some earlier theoretical speculation or prediction and could become another evidence for the “inverted” region of Marcus electron transfer model. The results could be very useful for materials design for developing high efficiency organic and polymer based optoelectronic devices; 2) Optimum LUMO offset or highest PL quenching appears much more critical than molar absorption coefficient for polymer-dye based optoelectronic conversion efficiency. 3) The optoelectronic performance of covalent attached polymer-dye system is much better than the polymer/dye blend system, this could be attributed to more convenient reach of polymer/dye interface of photo generated excitons in the covalent system resulting in more efficient exciton dissociations. 4) For thermoelectric studies, it appears the thermoelectric charge carrier generations of the four conjugated polymers doped with iodine at room temperature are in the normal region of the Marcus electron transfer model. An optimal thermoelectric charge generation condition may be identified with further decreasing the orbital offsets (D-HOMO/A-LUMO) of the D/A pairs or increasing the temperature, or both.

4.3 Student Training/Education/Publication Accomplishments

Though the project only budgeted/supported one graduate student, in reality, with leveraged supports from other sources, at least five graduate students (Two PhD levels and three Master levels) and several undergraduate students were trained and/or directly benefited as a result this project award, as these students are all part of the polymer research group contributing fully or partially on the project related research activities. Specifically, two PhD level students in polymer group successfully defended their PhD degree thesis already. One MS student who contributed to the thermoelectric studies defended her MS thesis and degree in December 2014, and another MS student defended his MS thesis in June 2015. Another graduate student has successfully passed all his PhD candidacy qualifying exams in summer 2015 is on the track toward a PhD degree. In addition to scientific journal publications, conference and invited seminar/lecture presentations, additional educational accomplishments include the preparation and submission (in July 2015) of the second edition of a graduate level textbook “*Introduction to Organic Electronic and Optoelectronic Materials and Devices*”, eds. S. Sun and L. Dalton, CRC Press/Taylor & Francis: Boca Raton, Florida, USA (1st edition ISBN-13: 978-0849392849), where four new chapters "Organic Spintronics", "Organic Thermoelectrics", "Organic Photo-actuators", and "Modeling" were added to the book second edition that is expected to be published during 2015-2016. Finally, a new textbook contract based on a new graduate level course titled "Materials and Devices for Solar Energy Conversions" (MSE-703) has been signed with Springer-USA and the textbook materials is currently under development and is planned to be published during 2016.

5. BIBLIOGRAPHY

- [1] S. Sun, and S. Sariciftci, eds., *Organic Photovoltaics: Mechanisms, Materials and Devices*, CRC Press, Boca Raton, Florida, **2005** (ISBN 0-82475-963-X).
- [2] Sun, S., "Optimal energy levels for organic donor/acceptor binary photovoltaic materials and solar cells", *Mater. Sci. & Eng., B*, **2005**, *116* (3), 251-256.
- [3] Sun, S., "Optimal Energy Offsets for Organic Solar Cells Containing a Donor/Acceptor Pair", *Sol. Energy Mater. Sol. Cells*, **2005**, *85*, 261-267.
- [4] Sun, S., "Chapter 3: Basic Electronic Structures and Charge Carrier Generation in Organic Optoelectronic Materials", in *Introduction to Organic Electronic and Optoelectronic Materials and Devices*, 2nd edition, Sun, S and Dalton, L eds., CRC Press/Taylor & Francis: Boca Raton, Florida, USA, in press, **2015**.
- [5] Sun, S.; Wang, D.; "Polymer Light Harvesting Composites for Optoelectronic Applications", *Nanophotonics and Macrophotonics for Space Environments XV, SPIE Proc.*, **2015**, Vol. 9616, accepted, in press.
- [6] Marcus, R. A. *J. Chem. Phys.* **1957**, *26* (4), 867.
- [7] Miller, J. R.; Calcaterra, L. T.; Closs, G. L. *J. Am. Chem. Soc.*, **1984**, *106*, 3047.